The role of heterogeneity on the development of excavation-induced fractures in the opalinus clay

Salina Yong
Engineering Geology, ETH Zurich, Zurich, Switzerland
Peter K. Kaiser[2], Simon Loew[1], Corrado Fidelibus[3]
[2]MIRARCO, Laurentian University, Sudbury, Ontario, Canada
[3]Bari Technical University, Bari, Italy

ABSTRACT
At the Mont Terri Rock Laboratory, research is undertaken to examine the suitability of the Opalinus Clay as a potential host rock for the deep geological disposal of nuclear waste. This paper examines the role of large-scale heterogeneity on the development of excavation-induced fractures mapped in the EZ-B field experiment. Rock mass and intact rock heterogeneity are compared by examining deviatoric stress contours from numerical simulations in conjunction with geological maps of the induced fractures. The analyses showed that if the tectonic shears were not kinematically constrained, mobilisation of the tectonic shears played a key role in the development of the mapped induced fractures.

RÉSUMÉ
Des études sont menées au laboratoire souterrain du Mont Terry pour déterminer l'adéquation des argiles à opalinus comme roche d'accueil pour un dépôt de déchets nucléaires profond. Le sujet de cet article est l'influence d'hétérogénéités préexistantes sur le développement de fractures induites par l'excavation de la niche EZ-B. Des comparaisons sont faites entre diverses modélisations des conditions de stress deviatorique après l'excavation de la niche, incluant les fractures antérieures à l'excavation ou non. Les résultats montrent qu'en fonction de l'orientation des fractures préexistantes par rapport au stress deviatorique, celles-ci sont réactivées par cisaillement ou non suite à l'excavation.

1 INTRODUCTION

At the Mont Terri Rock Laboratory in Switzerland (Figure 1), research is undertaken to investigate the potential of the Opalinus Clay as a host rock for deep geological disposal of high-level nuclear waste. The construction of an underground opening usually leads to the creation of an Excavation Damaged/Disturbed Zone or EDZ/EdZ (Tsang et al., 2005). Understanding the conditions under which fracturing is induced in the EDZ/EdZ is important in the context of geological waste repositories. Consideration of an overconsolidated argillaceous host adds mechanical complexities as these materials are inherently transitional and rarely isotropic.

It has been postulated that the EDZ/EdZ in the Opalinus Clay at the Mont Terri Rock Laboratory extends for 0.5-1 tunnel radii from the excavation periphery (Bossart et al., 2002). According to Martin et al. (2002), induced fracturing in the EDZ/EdZ consists of sidewall fractures oriented parallel with the tunnel axis and bedding-parallel fractures above the crown and below the invert.

Bedding in the Opalinus Clay at Mont Terri is ubiquitous and highly persistent leading to mechanical transverse isotropy. Adding to the complexity at the Rock Laboratory is the frequent occurrence of small-scale

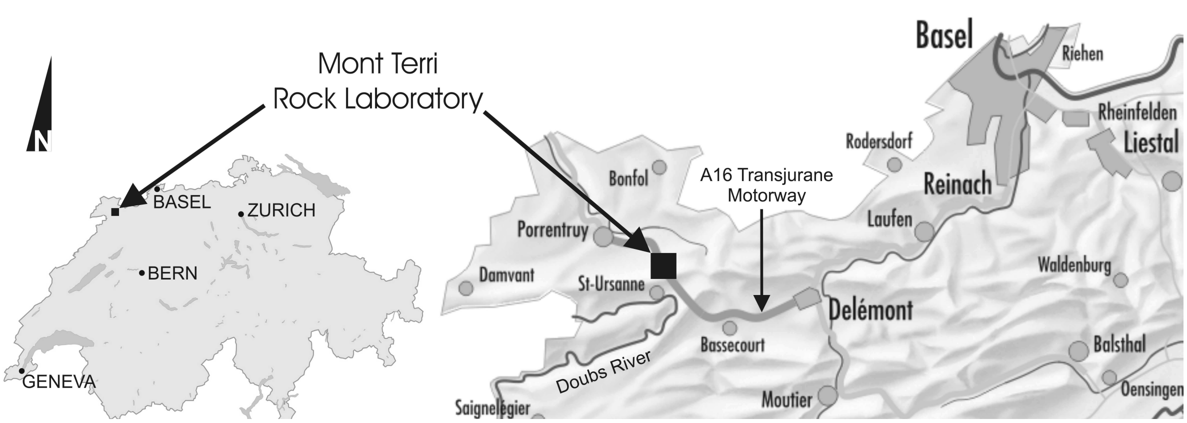

Figure 1. Location of the Mont Terri Rock Laboratory in northern Switzerland (modified from www.swisstopo.ch).

tectonic shears. At Mont Terri, much of the analyses have been focused on the bedding anisotropy owing to its prominent nature, which affects both mechanical properties of the rock and the development of the EDZ/EdZ. Consequently, little is known regarding the impact of the tectonic shears on the EDZ/EdZ. Observations made during a recent expansion of the laboratory indicated that the shears may have played an important role in the development of induced fracturing. A new 80m-long gallery (Gallery04) was excavated in 2004 with four adjoining niches that facilitated mapping of the damage caused by the gallery construction. This paper examines the role of intact rock heterogeneity versus rock mass heterogeneity (i.e. bedding-related versus that related to the tectonic shears) on the development of excavation-induced fractures mapped around Gallery04 in the vicinity of the one of the niches (EZ-B Niche).

2 SITE DESCRIPTION

Located northwest of Saint Ursanne (Figure 1), the Mont Terri Rock Laboratory consists of three galleries and a series of niches excavated adjacent to the A16 Transjurane Motorway tunnel. The laboratory was expanded in 2004 with the excavation of the 80m-long Gallery04. Gallery04 trends 262° for the first 30m then curves northwards to a final azimuth of about 300°. The site of interest is located in the straight stretch near the EZ-B Niche between tunnel metres (TM) 20 and 25 (Figure 2).

2.1 Geological Setting

Mont Terri is the northernmost in a series of anticlines in the Jura Mountains, which formed during late Miocene to early Pliocene in response to late alpine folding and thrusting (Homberg et al., 2005). Fault bend folding and fault propagation folding were responsible for the formation of the anticline and have resulted in a number of thrust faults, such as those found in the northern limb (Nussbaum et al., 2005b). The Rock Laboratory is located in the weakly deformed and less tectonically disturbed southern limb (Bath and Gautschi, 2003).

At Mont Terri, pervasive tectonic features include minor tectonic shears and a larger thrust fault zone (Nussbaum et al., 2005b; Bath and Gautschi, 2003). The tectonic shears are of minor tectonic importance with displacements in the order of millimetres (Nussbaum, pers. comm.) and require careful mapping. Three sets of shears have been identified in Gallery04 (Nussbaum et al., 2005b) but only two have been mapped near the EZ-B Niche (Nussbaum et al., 2005a). The most frequently occurring set is bedding-parallel and dips SSE (Nussbaum et al., 2005b). The SSE bedding-parallel shears are closed and sealed with calcite and clay minerals. Near the EZ-B Niche, the SSE shears dip 46° towards 146° (Nussbaum et al., 2005a); the niche trends roughly perpendicular to the SSE shears (Figure 2). A second set mapped in isolated areas of the niche (Nussbaum et al., 2005a) consists of sub-horizontal shears that dip S to SW (with dip angles ranging 0° to 20° and dip directions ranging 132° to 186°). In the niche, the sub-horizontal S-

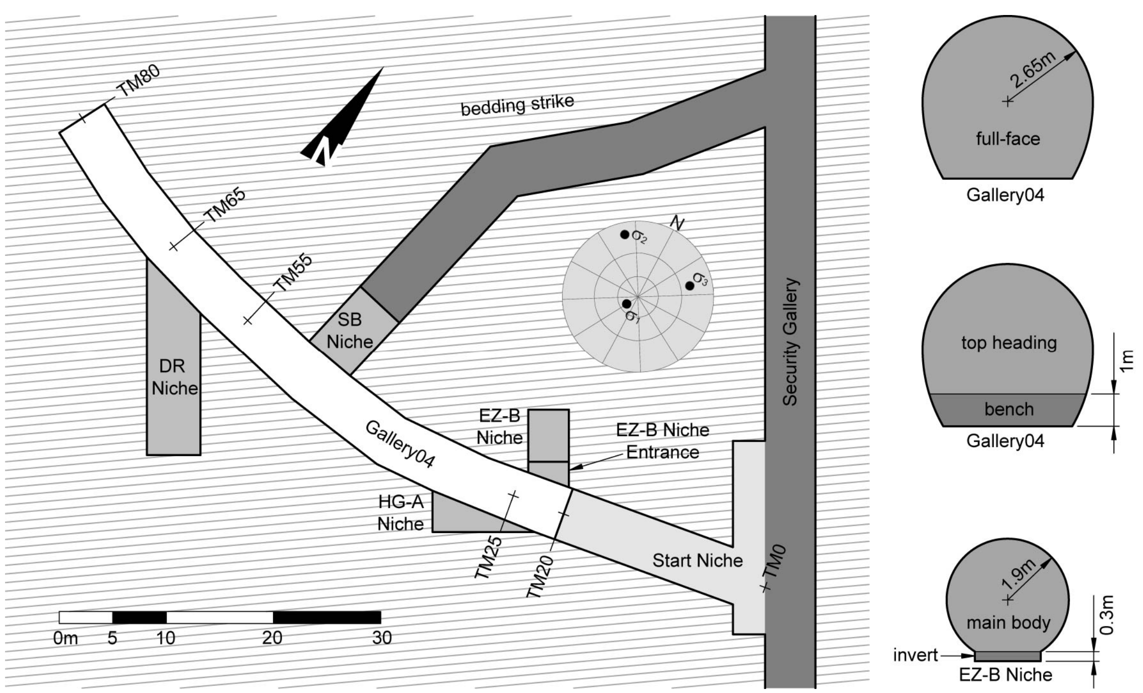

Figure 2. Layout of the Rock Laboratory around the EZ-B Niche and in situ stress field (lower hemisphere) with cross-sections of Gallery04 and the EZ-B Niche to the right.

SW shears are bounded by the SSE shears. The surfaces of both sets are slickensided and indicate thrusting towards the NW (Nussbaum et al., 2005b).

The Jurassic Opalinus Clay at Mont Terri is dark grey shale consisting of claystone and marl with intercalated sandy and calcareous layers and lenses. At Mont Terri, the formation consists of five lithostratigraphic subunits grouped into three facies (Gaucher et al., 2003): shaly, sandy, and carbonate-rich sandy. The major component of the shaly facies, where the Gallery04 and EZ-B Niche are located, consist of (Gaucher et al., 2003): clay minerals (58-76%), carbonates (0-28%), quartz (6-24%), feldspars (0-3%), pyrite (0-2%), and organic carbon (0-2%). Clay minerals consist mostly of illite (16-40% of total weight) and kaolinite (15-33%) followed by chlorite (4-20%) and illite/smectite mixed-layers (0-20%). The carbonate fraction is dominated by calcite at 5-28% (total weight). Structurally, the fabric is dominated by bedding-parallel flocculation; bedding is well-developed and the most pronounced feature at Mont Terri. Near the EZ-B Niche, bedding is millimetres thick with an average dip angle of 45° and dip direction of 147° (Nussbaum et al., 2005a); the niche trends approximately normal to the strike of bedding (Figure 2).

2.2 In Situ Stress

The in situ stress field (Table 1) at Mont Terri consists of a sub-vertical maximum principal stress (σ_1) inclined towards the S-SW and a sub-horizontal minimum principal stress (σ_3) inclined towards the NE (Bossart and Wermeille, 2003). Consequently, σ_3 is approximately normal to the axis of the EZ-B Niche while σ_2 (the intermediate principal stress) is sub-parallel with an offset of about 14° (Figure 2).

Table 1. In situ stress.

	Magnitude (MPa)	Dip Direction (°)/Dip (°)
σ_1	6-7	210/70
σ_2	4-5	320/10
σ_3	2-3	50/20

3 CONSTRUCTION OF GALLERY04

A road header and pneumatic hammer were utilised in the construction of Gallery04, which was excavated in three stages (Nussbaum et al., 2004; Nussbaum et al., 2005b). A 20m-long section (Start Niche) was first excavated under full-face conditions in March 2004 over a span of 25 days (Nussbaum et al., 2004). The final face of the Start Niche terminated near the east wall of the EZ-B Niche (TM20). The remaining length of Gallery04 was excavated in two stages (Nussbaum et al., 2005b): a top heading and a 1m-bench. The top heading was excavated continuously over a period of 58 days spanning August to October, 2004. The bench was excavated up to TM55 in eight days (28 October to 4 November, 2004) and stopped for the excavation of the SB and DR Niches. The bench excavation then re-commenced and was completed in an additional five days (25-29 November, 2004).

Support in Gallery04 (Nussbaum et al., 2005b) consisted of steel and fibreglass anchors (3m in length and 25mm in diameter) and steel- or fibre-reinforced shotcrete (15cm nominal thickness). In the first 20m, anchors were installed where bedding and/or the SSE shears were tangent to the gallery profile (between 9 o'clock and 11 o'clock, looking northwest). In the next 10m, anchors were installed between 9 o'clock and 12 o'clock. Prior to the invert excavation from TM20, anchors were also installed in both lower sidewalls. The last element of support was a 300mm-thick concrete floor slab, poured in two stages: TM20 to TM55 on 10 November, 2004 and the remaining 25m on 2 December, 2004.

4 FIELD OBSERVATIONS

Three sets of fractures induced by the construction of Gallery04 were mapped in the EZ-B Niche entrance (Figure 3). The most commonly mapped system (IF1) is oriented sub-parallel with the gallery while fractures oblique (IF2) to the gallery axis are the least often mapped as these were specifically sought after in the EZ-B Experiment (Yong et al., 2006). The third system (IF3) is sub-parallel with bedding and is limited to the perimeter of the gallery. The focus of this paper (as of most investigations) is on the IF1 extensional fractures.

In the EZ-B Niche entrance, IF1 fractures were mapped in two different orientations (Figure 3). In the west wall, IF1 fractures were sub-perpendicular to the SSE shears (and therefore, also bedding). In the east wall, IF1 fractures were sub-parallel with the wall of Gallery04.

Understanding the difference in the IF1 orientations between the west and east niche walls requires returning to the site description and the geological setting (Figure 2). For the first 30m, Gallery04 trends about 25°-30° from the strike of the SSE shears. The SSE shears in the vicinity of the EZ-B Niche have an average dip of 46° and an average dip direction of 146°. Consequently, shears that intersected Gallery04 in the west wall did not necessarily intersect the gallery in the east wall. For example, F5 and F7 daylighted in Gallery04 in the west niche wall but neither daylighted in the east niche wall (Figure 3). In addition, S-SW shears daylighted in the east wall whereas those in the west wall did not. This led to greater kinematic freedom where F5 and F7 daylighted in the west wall and where the S-SW shears, F1, F2, and F3 daylighted in the east wall. Thus, the distinct difference between the two walls was the kinematic freedom or lack of shear constraint of the S-SW shears. As a result, it was speculated that only the SSE shears were mobilised in the west wall while mobilisation of the S-SW shears interfered with mobilisation of the SSE shears in the east wall. In this case, IF1 fracturing would be nearly perpendicular to the most mobilised shear in both walls. This hypothesis is tested in the following section.

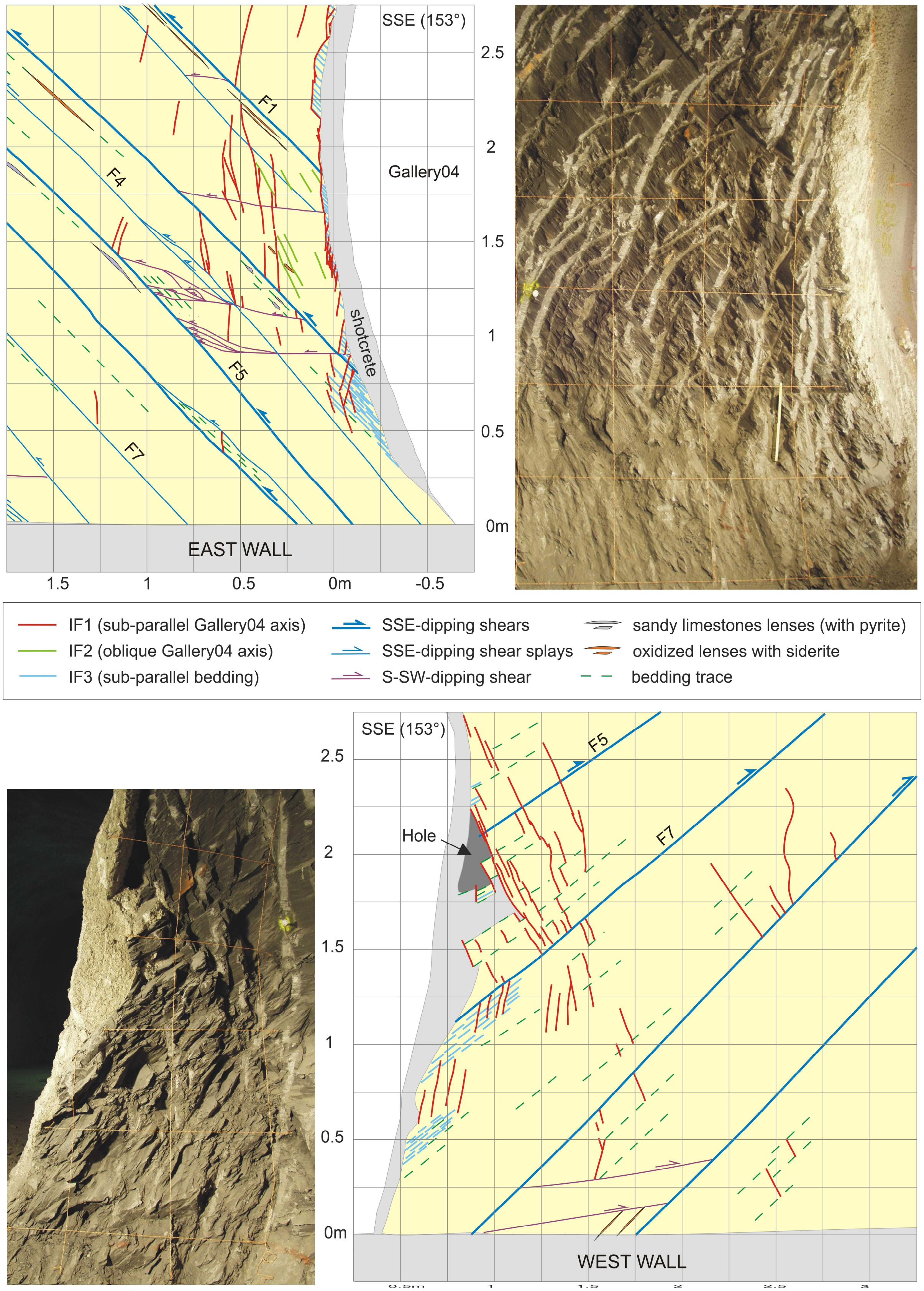

Figure 3. Induced fracturing in the east (top) and west (bottom) walls in the EZ-B Niche entrance (geological maps modified from Nussbaum et al., 2005a).

5 ROLE OF HETEROGENEITY ON INDUCED FRACTURING

Two-dimensional continuum numerical modelling was undertaken to examine the influence of the tectonic shears on the induced fractures mapped in the entrance of the EZ-B Niche entrance. Phase2 (Rocscience, 2005) was used in these analyses.

5.1 Estimating Properties for Tectonic Shears

Mechanical properties of the Opalinus Clay at Mont Terri have been determined from laboratory testing on intact rock samples. However, the mechanical properties of the tectonic shears are unknown. As a first approximation, an elasto-plastic back-analysis was first carried out in Phase2 (Yong, 2007). To demonstrate the influence of the tectonic shears on induced fracturing, elastic analyses were undertaken to fulfill the objectives of this paper.

Stiffness values of the tectonic shears were estimated according to Barton (1972). Given the rock mass modulus (E_{rm}) along with the intact rock modulus (E_i) and the spacing between joints (L), the normal stiffness was obtained via:

$$k_n = E_i E_{rm}/L(E_i - E_{rm}) \qquad [1]$$

Likewise, given the equivalent shear moduli (G), the shear stiffness was obtained via:

$$k_s = G_i G_{rm}/L(G_i - G_{rm}) \qquad [2]$$

The average spacing of the tectonic shears in the vicinity of the niche was about 1m. The intact rock moduli were known from Bock (2001) but not the rock mass moduli. As a result, the rock mass modulus was estimated based on the intact unconfined compressive strength (σ_{ci}), GSI, and disturbance factor (D) according to Hoek et al. (2002):

$$E_{rm}\ (\text{GPa}) = (1 - D/2)(\sigma_{ci}/100)^{1/2}10^{((GSI-10)/40)} \qquad [3]$$

The GSI for the Opalinus Clay at Mont Terri was estimated to range between 40 and 50 (blocky structure and fair to poor surface conditions), after Marinos and Hoek (2000). This represented a reduction of roughly 50% in the intact modulus (k_n = 4GPa/m and k_s = 1.5GPa/m). Although the stiffness values inferred in this manner are largely approximated and constant, the objective of this paper is to show the possible influence of the tectonic shears on the induced fracturing mapped in the EZ-B Niche entrance.

5.2 Modelling Heterogeneity

Owing to the asymmetry of the alignment of Gallery04 with the strike of bedding and the SSE shears, two plane-strain models were built with one representing the west niche wall and one representing the east wall. Construction of Gallery04 was simulated in two steps with excavation of the top heading in the first followed by excavation of the bench (Figure 2). The external boundary was fixed in all directions and located about 40m from the gallery boundary (or more than seven tunnel diameters). The SSE shears were modelled as continuous joints with a dip angle of 46°. The in-plane stress field consisted of σ_1 at 7MPa inclined 20° from vertical (Figure 2) and σ_2 as the minimum principal stress at 4MPa. The out-of-plane stress consisted of σ_3 at 2MPa.

In the elastic analyses, two scenarios were examined to assess the impact of rock heterogeneity on the modelled results in comparison with field observations. The first scenario considered only the intact rock (i.e. no joints) while both the SSE and S-SW shears were considered in the second. Additionally, two matrix conditions were compared in each scenario (Table 2). The first considered an isotropic rock matrix (Figure 4) while the second considered a transverse isotropic (or anisotropic) rock matrix (Figure 5). In the latter case, the bedding anisotropy was represented with the isotropic plane inclined 45° from horizontal. Three deviatoric stress iso-lines are shown in the figures. The 10MPa iso-line (in white) corresponds to σ_c (unconfined compressive strength) at a loading direction parallel with bedding while the 16MPa iso-line (in black) corresponds to σ_c at a loading direction perpendicular to bedding (Bock, 2001). The 8MPa iso-line was included since it best captured the zone of induced fracturing.

Table 2. Properties used in the numerical analyses.

	Isotropic	Anisotropic
$E_{bedding\ parallel}$ (GPa)	6	10
$E_{bedding\ perpendicular}$ (GPa)		4
$\nu_{bedding\ parallel}$	0.27	0.33
$\nu_{bedding\ perpendicular}$		0.24
k_n (GPa/m)	4	4
k_s (GPa/m)	1.5	1.5

In the first scenario (i.e. no joints), matrix anisotropy (shown in the right of Figure 4) resulted in deviatoric stress localisation where bedding is nearly tangential to the perimeter of Gallery04. In the second scenario (Figure 5), the tectonic shears were modelled as elastic elements but with stiffness values equivalent to those used in the plastic back-analysis (Table 2). Interestingly, the three deviatoric stress iso-lines differ only slightly between the isotropic matrix case (shown in the left of Figure 5) and the anisotropic matrix case (shown in the right of Figure

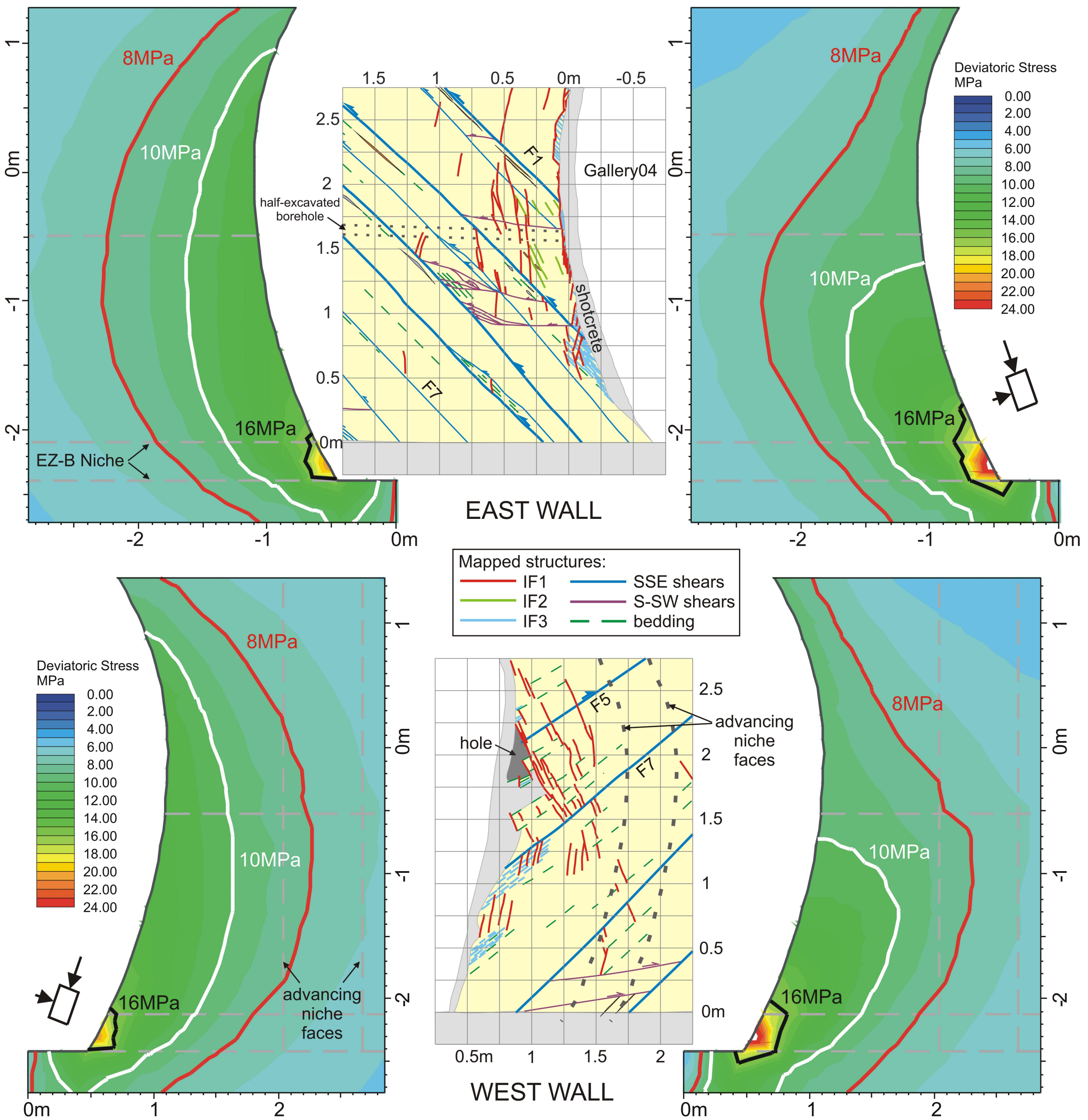

Figure 4. Deviatoric stress contours of elastic isotropy (left) compared to elastic transverse isotropy (right) without consideration of the tectonic shears. East niche entrance wall in the top and west niche entrance wall in the bottom.

5). In the west wall, the S-SW shears had little impact on the stress contours near the gallery wall; hence, the stress contours remained roughly normal to the SSE shears. In the east wall, mobilisation of the S-SW shears interfered with the mobilisation of the SSE shears. As a result, stress contours became normal to the S-SW shears or parallel with the gallery wall. These results implied that the SSE shears were mobilised without interference from the S-SW shears in the west wall. In contrast, mobilisation of the S-SW shears interfered with the mobilisation of the SSE shears in the east wall.

6 CONCLUSIONS

Understanding the conditions under which fracturing is induced in the EDZ/EdZ is important in the context of geological nuclear waste disposal. Consideration of an overconsolidated argillaceous host adds mechanical complexities as these materials are inherently transitional and rarely isotropic. The Opalinus Clay at the Mont Terri Rock Laboratory is characterised by pronounced bedding and frequently-occurring small-scale tectonic shears. Much focus in the past has been on the intact rock

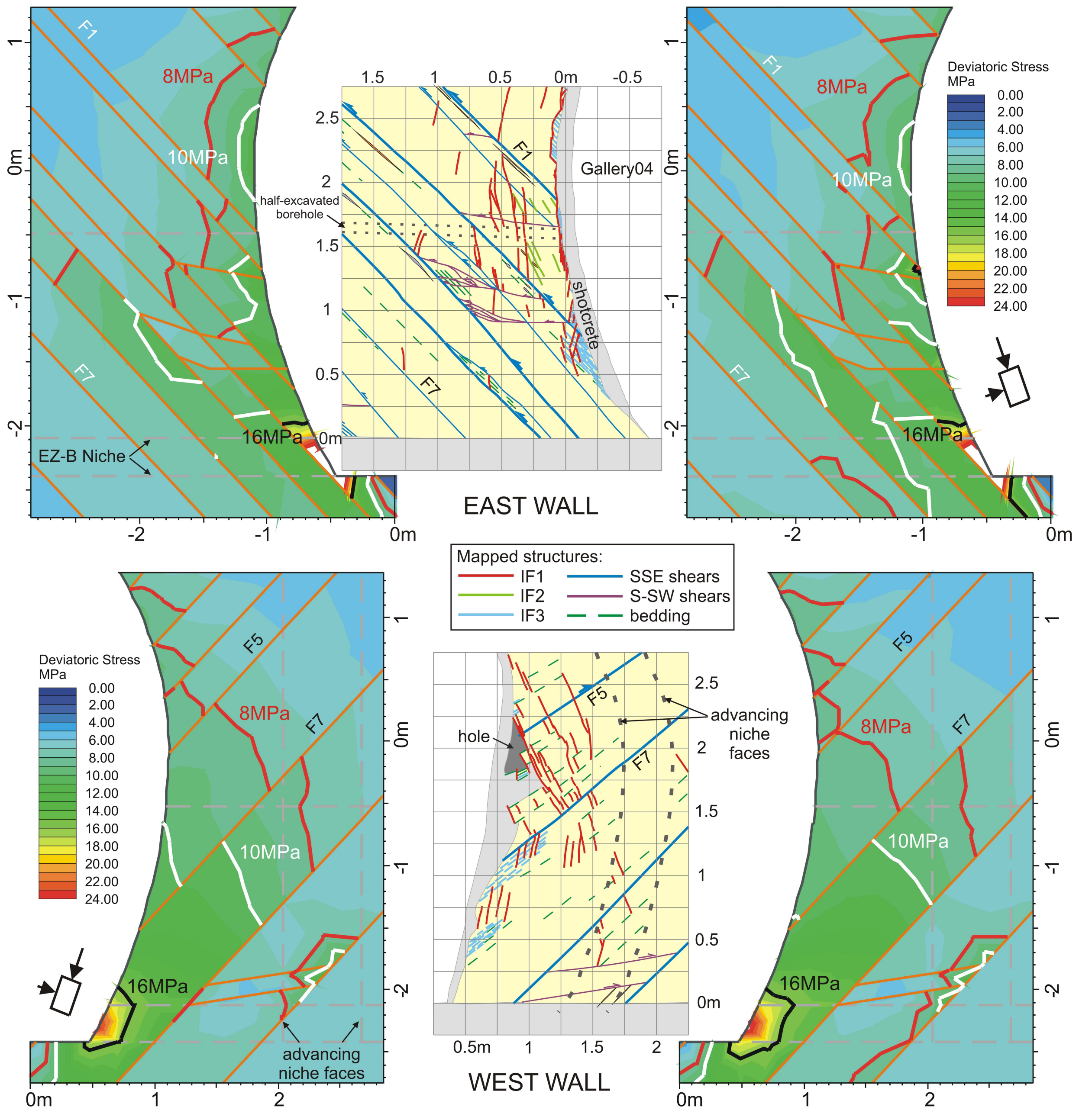

Figure 5. Deviatoric stress contours of elastic isotropy (left) compared to elastic transverse isotropy (right) with all mapped shears modelled. East niche entrance wall in the top and west niche entrance wall in the bottom.

heterogeneity (i.e. bedding). In this paper, consideration was also given to the tectonic structures thereby allowing for rock mass heterogeneity to be accounted for.

Geological mapping of excavation surfaces during a recent expansion of the facility has shown that minor tectonic shears, which can be easily overlooked, influence induced fracturing. In the west wall of the EZ-B Niche entrance, the SSE bedding-parallel shears were mobilised without interference from the sub-horizontal S-SW shears. In this case, induced fractures propagated sub-perpendicular to the SSE shears. In the east wall, mobilisation of the S-SW shears interfered with the mobilisation of the SSE shears inducing fracture growth in a direction that was parallel with the gallery wall.

The results showed that when the tectonic shears are accounted for (i.e. more deformable than the surrounding matrix), the stress field was influenced in a similar manner whether or not the intact rock matrix was isotropic or anisotropic. This implied that the rock mass anisotropy (i.e. due to the tectonic shears), rather than the intact rock matrix anisotropy (i.e. due to the bedding), dominated in the development of the induced fractures mapped in the EZ-B Niche entrance.

ACKNOWLEDGEMENTS

The Swiss Nuclear Safety Inspectorate (HSK) provided the funding for this project, and Dr. Erik Frank in particular is thanked for his support. Special thanks to Drs. Christophe Nussbaum and Frank Lemy for providing the geological mapping and corresponding photographs. Translation of the abstract into French was provided by Olivier Masset.

REFERENCES

Barton N.R. 1972. A model study of rock-joint deformation, *International Journal of Rock Mechanics & Mining Sciences*, 9:579-602.

Bath A. and Gautschi A. 2003. Geological setting and sample locations, *Reports of the Federal Office for Water and Geology*, Geology Series No.5, pp.30-35.

Bock H. 2001. RA experiment rock mechanics analyses and synthesis: data report on rock mechanics, *Unpublished Mont Terri Technical Report*, 52pp.

Bossart P. and Wermeille S. 2003. The stress field in the Mont Terri region data compilation, *Reports of the Federal Office for Water and Geology*, Geology Series No.4, pp.65-92.

Bossart P., Meier P.M., Moeri A., Trick T., and Mayor J.-C. 2002. Geological and hydraulic characterisation of the excavation disturbed zone in the Opalinus Clay of the Mont Terri Rock Laboratory, *Engineering Geology* 66:19-38.

Gaucher E.C., Fernandez A.M., and Waber H.N. 2003. Rock and mineral characterisation of the Opalinus Clay Formation, *Reports of the Federal Office for Water and Geology*, Geology Series No.5. pp.281-303.

Hoek E., Carranza-Torres C., and Corkum B. 2002. Hoek-Brown failure criterion - 2002 edition, *NARMS-TAC 2002*, University of Toronto Press; Toronto, ON, CA, 1:.267-273.

Homberg C., Bergerat F., Philippe Y., Lacombe O., and Angelier J. 2005. Structural inheritance and cenozoic stress fields in the Jura fold-and-thrust belt (France), *Tectonophysics* 357:137-158.

Jaeger J.C. 1960. Shear failure of anisotropic rocks, *Geological Magazine*, 97:65-72.

Marinos P.and Hoek E. 2000. GSI: a geologically friendly tool for rock mass strength estimation, *GeoEng 2000*, Technomic Publishing Co., Melbourne, Australia, 1:1422-1440.

Martin C.D., Lanyon G.W., Bluemling P., and Mayor J.-C. 2002. The excavation disturbed zone around a test tunnel in the Opalinus Clay, *NARMS-TAC 2002*, University of Toronto Press; Toronto, ON, CA,. 2:1581-1588.

McLamore R. and Gray K.E. 1967. The mechanical behavior of anisotropic sedimentary rocks, *Journal of Engineering for Industry*, 89:62-73.

Nussbaum C., Bossart P., Burrus F., Jeannin P.Y., and Graf A. 2004. Survey and documentation of the Start Niche excavation, *Unpublished Mont Terri Technical Note*. 26pp.

Nussbaum C., Bossart P., von Ruette J., Meier O., and Badertscher N. 2005a. EZ-B experiment: small-scale mapping of tectonic and artificial (EDZ) fractures of the EZ-B niche, *Unpublished Mont Terri Technical Note*, 23pp.

Nussbaum C., Bossart P., Burrus F., Badertscher N., Meier O., and Nold A. 2005b. Excavation of Gallery04: general documentation, deformation measurements and geological surveys, *Unpublished Mont Terri Technical Note*, 87pp.

Rocscience Inc. 2005. Phase2 version 6.0 - finite element analysis for excavations and slopes, *www.rocscience.com*.

Tsang, C.-F., Bernier, F., and Davies, C. 2005. Geohydromechanical processes in the Excavation Damaged Zone in crystalline rock, rock salt, and indurated and plastic clays-in the context of radioactive waste disposal, *International Journal of Rock Mechanics & Mining Sciences* 42:109-125.

Yong S. 2007. A three-dimensional analysis of excavation-induced perturbations in the Opalinus Clay at the Mont Terri Rock Laboratory, PhD thesis, *ETH Zurich*, 180pp.

Yong S., Loew S., Fidelibus C., Frank E., Lemy F., and Schuster K. 2006. Induced fracturing in the Opalinus Clay: an integrated field experiment, 4th Asian Rock Mechanics Syposium, World Scientific, Singapore, CD-Rom. 9pp.